Case Studies in Construction Materials 21 (2024) e03850

Contents lists available at ScienceDirect

Case Studies in Construction Materials

journal homepage: www.elsevier.com/locate/cscm

Adhesion performance and enhancement mechanism of FA/GGBFS based geopolymer modified bitumen and acidic aggregate

Wenjie Du [a], Ning Tang [a,*], Yihan Sun [b], Nan Nie [a], Ruofei Zhang [a], Ke Wang [a]

[a] School of Materials Science and Engineering, Shenyang Jianzhu University, Shenyang 110168, China
[b] Zhejiang Scientific Research Institute of Transport, Hangzhou 310023, China

ARTICLE INFO

Keywords:
Bitumen
Geopolymer
Acidic aggregate
Adhesion

ABSTRACT

The primary challenge in utilizing acidic aggregates in bitumen mixtures lies in enhancing the adhesive bond between the bitumen and the acidic aggregates. In this manuscript, to investigate the adhesion of different geopolymer modified bitumen with acidic aggregates, fly ash geopolymer (FG), fly ash- ground granulated blast furnace geopolymer (SFG), and ground granulated blast furnace (SG) were prepared by fly ash (FA), ground granulated blast furnace (GGBFS) with alkali activator. The different geopolymers were characterized with SEM, XRD, FTIR. Different geopolymer modified bitumen was prepared by adding geopolymers into virginal bitumen. The conventional properties, viscosity, and rheological properties of modified bitumen were measured and analysed. The adhesion of bitumen to acidic aggregates was tested by Zeta potential test, the improved boiling water test and pull-off test. The results showed that the electronegativity of bitumen and acidic aggregates were weakened significantly by Na^+ in skeletal structure of fly ash geopolymer. The high temperature stability of fly ash geopolymer modified bitumen was improved and the bond strength of bitumen with acidic aggregates increased remarkably with the addition of 9 % fly ash geopolymer.

1. Introduction

Bitumen mixtures are composite materials consisting of bitumen, coarse aggregates, fine aggregates and fillers [1,2]. Alkaline aggregates and neutral aggregates are often used in bitumen mixtures, while acidic aggregates are not used in bitumen mixtures due to their poor adhesion to bitumen [3,4]. The demand for sand and gravel resources for infrastructure construction is increasing with the acceleration of global urbanization, and there is a shortage of alkaline and neutral aggregates, while acidic aggregates with high strength and excellent abrasion resistance have a wide range of application prospects in bitumen mixtures [5–7]. Therefore, it is a focus of current research in road engineering to improve the adhesion of bitumen to acidic aggregates and reduce the water stability of bitumen mixture [8,9].

The application of amine anti-stripping additives has become an effective measure to enhance the adhesion between bitumen and acidic aggregates in recent years. Polar molecules in the anti-stripping additives combine with acidic aggregates, and non-polar molecules combine with bitumen, which can improve the adhesion between bitumen and acidic aggregates effectively [9–11]. In addition, it has been found that wrapping aggregates with cement, slaked lime and substituting fillers in bitumen mixtures can effectively enhance the adhesion of bitumen to acidic aggregates [12–15]. However, amine anti-stripping additives are easily

* Corresponding author.
E-mail address: tangning@sjzu.edu.cn (N. Tang).

https://doi.org/10.1016/j.cscm.2024.e03850
Received 24 June 2024; Received in revised form 5 September 2024; Accepted 11 October 2024
Available online 14 October 2024

decomposed at high temperature and slaked lime in bitumen mixtures expands easily under the attack of water, in addition that the efficiency of wrapping acidic aggregates with cement and slaked lime is low [16,17]. Geopolymer has a broad application prospect in construction and transportation as a new and environmentally friendly inorganic cementitious material [18]. Sri Atmaja P. Rosyidi et al. [19] prepared geopolymer modified bitumen by adding fly ash geopolymer to bitumen, and the study found that fly ash geopolymer modified bitumen has reduced the contact angle with aggregates and the adhesion between bitumen and aggregates has improved. Meng et al. [20] added geopolymer which was prepared by metakaolin, ground granulated blast furnace, and silica fume to bitumen, the study indicated that the addition of geopolymer into bitumen improved the adhesion of bitumen to aggregates. Therefore, geopolymer has great application prospects in bitumen mixture.

Geopolymer is a new inorganic cementitious material obtained by industrial solid wastes such as fly ash (FA), ground granulated blast furnace powder (GGBFS), silica fume (SF) and metakaolin (MK) under the activation of alkali medium [21–23]. The reaction products of geopolymer are different due to the different raw materials. Low calcium fly ash, metakaolin, etc. form N-A-S-H gel (NaOH, sodium silicate solution alkali activator) and K-A-S-H gel (KOH alkali activator) with the addition of alkali activator, while ground granulated blast furnace powder and high calcium fly ash form C-(A)-S-H gel [24–27].

Different products of geopolymer reaction have different effects on the properties of geopolymer modified bitumen. This work investigates the effect of different reaction products of geopolymer on the adhesion of bitumen to acidic aggregates, providing support for the application of acidic aggregates in bitumen mixtures.

2. Materials and methods

2.1. Materials

2.1.1. Geopolymer

Fly ash geopolymer (FG), fly ash and ground granulated blast furnace geopolymer (SFG), and ground granulated blast furnace geopolymer (SG) were prepared by mixing FA and GGBFS with alkaline activator and water respectively, in which the alkaline activator is made by mixing water glass, sodium hydroxide and water. FA (I) and GGBFS (S95) are provided by Longze Water Purification Materials Co., Ltd. (Henan, China) and the chemical composition of GGBFS and FA is shown in Table 1. Water glass is liquid sodium silicate (Na_2O:8.3 %, SiO_2:26.5 %) produced by Shandong Yousuo Chemical Technology Co., Ltd. Sodium hydroxide (NaOH $\geq$ 96 %) was supplied by Tianjin Hengxing Reagent Co., Ltd.

2.1.2. Aggregates

Acidic aggregates are granite aggregates provided by Zhejiang Communications Resources Investment Group Co., Ltd. (Zhejiang, China), and the chemical composition of the aggregate is shown in Table 1.

2.1.3. 2.1.3 Bitumen

70# virginal bitumen was provided by Zhejiang Communications Resources Investment Group Co., Ltd. (Zhejiang, China). The conventional properties of bitumen are displayed in Table 2 and conform to the Chinese specification JTG E20–2011.

2.2. Geopolymer: preparation and tests

2.2.1. Geopolymer preparation

FG, SFG, and SG were prepared by FA and GGBFS. Fig. 1 shows the preparation of geopolymer additives.

(1) 3.70 g sodium hydroxide and 36.30 g sodium silicate (water glass modulus: 1.4) were mixed and dissolved to obtain an alkali activator.

(2) FA and GGBFS were weighed in the proportion (FA: GGBFS=100:0; FA: GGBFS=30:70; FA: GGBFS=0:100) of 100 g and mixed with 40 g of alkali activator and 10 g of water (liquid to solid ratio of 0.5), to obtain the geopolymer slurry, which was poured into the molds and covered with plastic film.

(3) Geopolymer was cured at ambient temperature for 24 h and then demolded and placed in the standard curing room (temperature: 20±2℃, humidity: ≥95 %) for curing until 72 h.

(4) The geopolymer was milled into particles leaving particles smaller than 75 μm. The particles were dried at 200℃ for 4 h to reduce the effect of moisture on the adhesion of modified bitumen to acidic aggregates.

2.2.2. Scanning electron microscopy (SEM)

SEM can characterize the microscopic morphology of materials [28]. The microscopic morphology of FG, SFG and SG was

Table 1
Chemical composition of raw materials.

Chemical composition	SiO_2	Al_2O_3	CaO	SO_3	Fe_2O_3	K_2O	MgO	Na_2O
GGBFS/%	34.50	17.70	34.50	1.64	1.03	-	6.01	-
FA/%	53.97	31.15	4.01	0.73	4.16	-	1.01	-
Granite/%	65.26	18.58	4.96	-	2.84	2.96	4.00	1.40

Table 2
Properties of 70# virginal bitumen.

Property	Unit	Result	Technical requirements	Test
Penetration	dmm	67	60–80	T0604
Ductility	cm	22.6	≥20	T0605
Softening point	℃	48.0	≥46	T0606
Density	g/cm^3	1.037	1.01	T0603

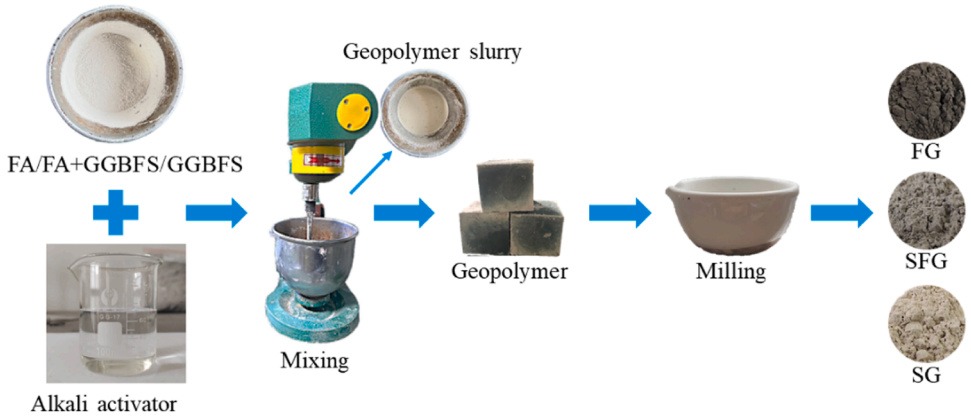

Fig. 1. Preparation of geopolymer additives.

compared and analyzed using SEM manufactured by ZEISS (Germany).

2.2.3. X-ray diffractometry (XRD)

XRD can analyze the physical phase of materials [29]. The physical phase composition of FG, SFG, and SG was analyzed using an X-ray diffractometer manufactured by Shimadzu (Japan) with scanning speed of 5°/min and scanning angles 10°-90°.

2.2.4. Fourier transform infrared spectroscopy (FTIR)

FG, SFG, and SG were analyzed using a Fourier infrared spectrum analyzer manufactured by Nicolet (American) with a scanning range of 400 cm^{-1} to 4000 cm^{-1}.

2.2.5. Zeta potential

The Zeta potential of geopolymer (FG, SFG and SG) at different pH values were employed by a NanoPlus particle analyzer (American). 1.0 g geopolymer (FG, SFG and SG) was added to solutions and solutions of different pH values (3, 5, 7, 9, 11) were prepared by adding NaOH and HCl to deionized water.

2.3. Geopolymer modified bitumen: preparation and tests

2.3.1. Geopolymer modified bitumen preparation

The 70# virginal bitumen was kept at 135℃ for 1.5 h, then the particles of geopolymer (3 %, 6 %, 9 %, 12 % of the bitumen mass)

Table 3
Blending ratios and labels of different modified bitumen.

Types	Additives	Label	The ratio of additives to the weight of bitumen
FMB	FG	F3	3 %
		F6	6 %
		F9	9 %
		F12	12 %
SFMB	SFG	SF3	3 %
		SF6	6 %
		SF9	9 %
		SF12	12 %
SMB	SG	S3	3 %
		S6	6 %
		S9	9 %
		S12	12 %

were added to bitumen and stirred with a high-speed shearer (2000r/min, 30 min). Geopolymer modified bitumen was obtained by cooling at ambient temperature. Blending ratios and labels of different modified bitumen are shown in Table 3.

2.3.2. Conventional properties of bitumen

The penetration, softening point, ductility and viscosity at 135℃ of geopolymer modified bitumen were tested, following the Chinese specification JTG E20–2011.

2.3.3. Rheological properties of bitumen

The rheological properties of bitumen were tested using temperature sweep. The test temperature was 46–82°C with a temperature gradient of 6°C, and the frequency was 1.59 Hz.

2.3.4. Boiling water test

The adhesion of acidic aggregates to bitumen was tested using the improved boiling water test due to the ambiguous temperature of the traditional boiling water test [30]. Firstly, the bitumen was wrapped around the acidic aggregates which were kept immersed in heated bitumen (163°C) for 45 s. Then, the acidic aggregate wrapped with bitumen was cooled at ambient temperature for 15 min. Finally, the acidic aggregates wrapped with bitumen were immersed in the same depth of water (90°C±1℃) for the improved boiling water test with 3 minutes. Fig. 2 displays the process of boiling water test.

Acidic aggregates were photographed by a camera. The pictures were imported into the software of "Photoshop" and the areas of stripping bitumen on the aggregate surface were covered with "red" (Fig. 2 (C) shows before and after treatment of acidic aggregates). In addition, the stripping area was selected using "Image recognition" (Fig. 2(D)), and the number of pixels in the stripping area was obtained using the "Histogram" function (number of pixels in the red area in Fig. 2(E)). And based on the ratio of pixels of the stripping area to the acidic aggregate, the stripping area of bitumen could be accurately obtained.

2.3.5. Pull-off test

The pull-off test was carried out to evaluate the adhesion of bitumen to acidic aggregates [31]. A granite cube of 40 mm×40 mm×40 mm was used for the pull-off test. According to the relationship between bitumen and film thickness of bitumen, bitumen was applied to the granite cube and a certain pressure was applied to the granite cube to ensure the bitumen film thickness between the two granite cubes was 200 μm, and removed the excess bitumen. The samples of the pull-off test were cooled at ambient temperature for 24 hours to be used [32]. Fig. 3 shows samples preparation and test procedures of pull-off test.

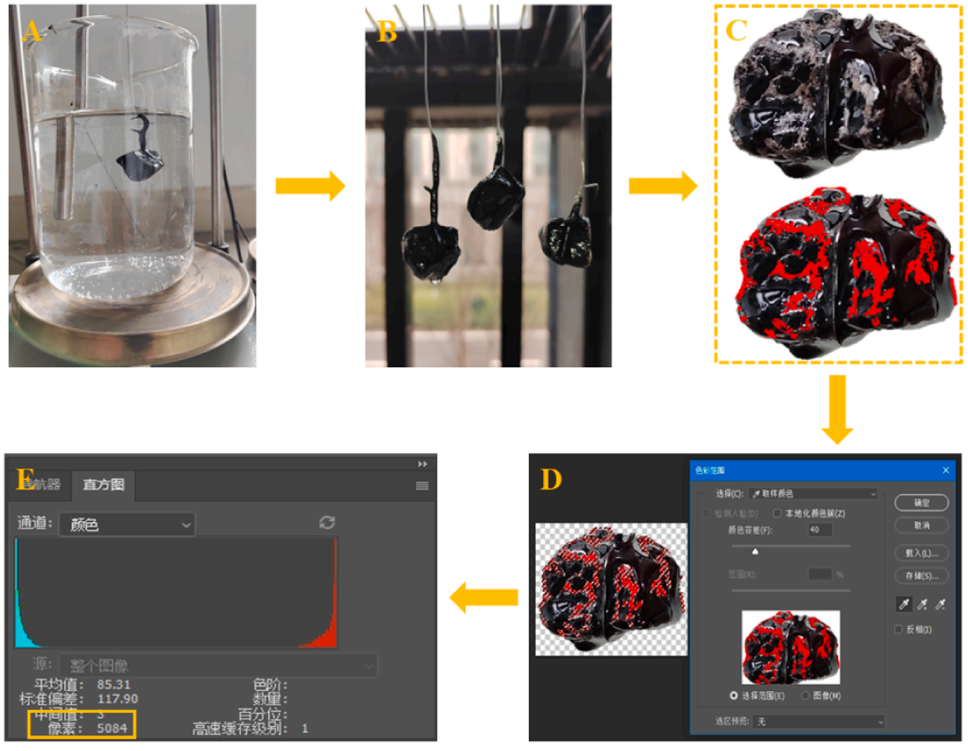

Fig. 2. The process of boiling water test. (A: Boiling water test, B: Aggregates after boiling water test, C: Image processing, D: Colour recognition, E: Pixels of different colours).

3. Results and discussion

3.1. Characteristics of geopolymer

3.1.1. SEM

Fig. 4 shows the microstructural image of FG, SFG, and SG. As can be seen from Fig. 4 (A) (D), a large amount of N-A-S-H gel was generated on the surface of FA particles with the addition of alkali activator [33]. It can be seen from Fig. 4 (B) (E) that FA and GGBFS particles were wrapped with C-(A)-S-H gel and N-A-S-H gel when FA and GGBFS reacted with alkali activator. However, the gel in Fig. 4 (B) (E) is dominated by N-A-S-H gel, with relatively few C-(A)-S-H gel, due to the decomposition of C-(A)-S-H gel under high temperature [34]. As can be seen from Fig. 4 (C) (F), GGBFS particles generated C-(A)-S-H gel in the presence of alkali activator, and the residual granular C-(A)-S-H gel wrapped with GGBFS particles due to the decomposition under high temperature [35]. In contrast to FG, SFG, and SG, C-(A)-S-H gel decreased and the surface of geopolymer particles became smooth with the increasing content of GGBFS.

3.1.2. XRD

Fig. 5 shows the XRD pattern of FG, SFG, and SG. As can be seen from Fig. 5, there is a diffuse peak between 20° and 40°. The main components of FA are SiO_2 and Al_2O_3, which produce N-A-S-H gel with the addition of alkali activator. FA contains quartz, mullite, and corundum which are considered to be inert and unreacted in the alkaline environment [33,36]. C-(A)-S-H gel was generated in the presence of alkali activator due to GGBFS containing CaO and Al_2O_3, as a result, SFG and SG appeared amorphous substances on the XRD pattern and did not show significant diffraction peaks.

3.1.3. FTIR

Fig. 6 displays the FTIR spectra of FG, SFG, and SG. The peaks at 3200 cm-1–3600cm^{-1} were caused by stretching vibration of OH-, which can reflect the degree of reaction of the geopolymer [37]. A bending vibrational peak of H-O-H at 1629 cm^{-1} indicates that water is in geopolymer. The peak at 1400 cm^{-1} was related to C═O indicating carbonation of the alkali activator which reacted incompletely [38]. There was asymmetric stretching vibration at 900 cm^{-1}-1250cm^{-1}, which was mainly due to the hydration products of geopolymer [39]. The peak at 462 cm^{-1} was related to the bending vibration and stretching vibration of the TO_4^{2-} tetrahedron (T=Si or Al) [40].

3.2. Performance of modified bitumen

3.2.1. Conventional performances of modified bitumen

Fig. 7 shows the conventional properties of modified bitumen ((A): Penetration, (B): Softening point, (C): Ductility, (D): Viscosity at 135℃). As can be seen from Fig. 7, the conventional properties of modified bitumen changed significantly with the addition of geopolymer. A stable network structure was formed in the bitumen when the geopolymer was added to the bitumen, which restricted the movement of the bitumen molecular chains. As a consequence, the bitumen hardened and the plasticity increased. The penetration and ductility of FMB were lower than SFMB and SMB and the softening point was higher than SFMB and SMB when the addition of geopolymer was 3 %. However, with the increase of geopolymer addition, there was no significant difference in penetration, ductility,

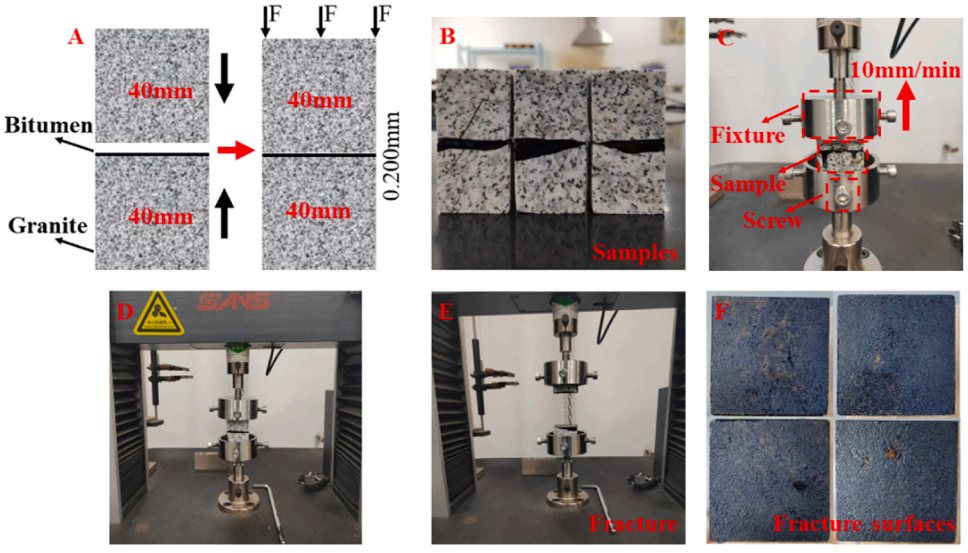

Fig. 3. Pull-off test: samples preparation and test procedures. (A: Samples preparation, B: Samples, C: Fixture, D, E: Testing, F: Fracture surfaces).

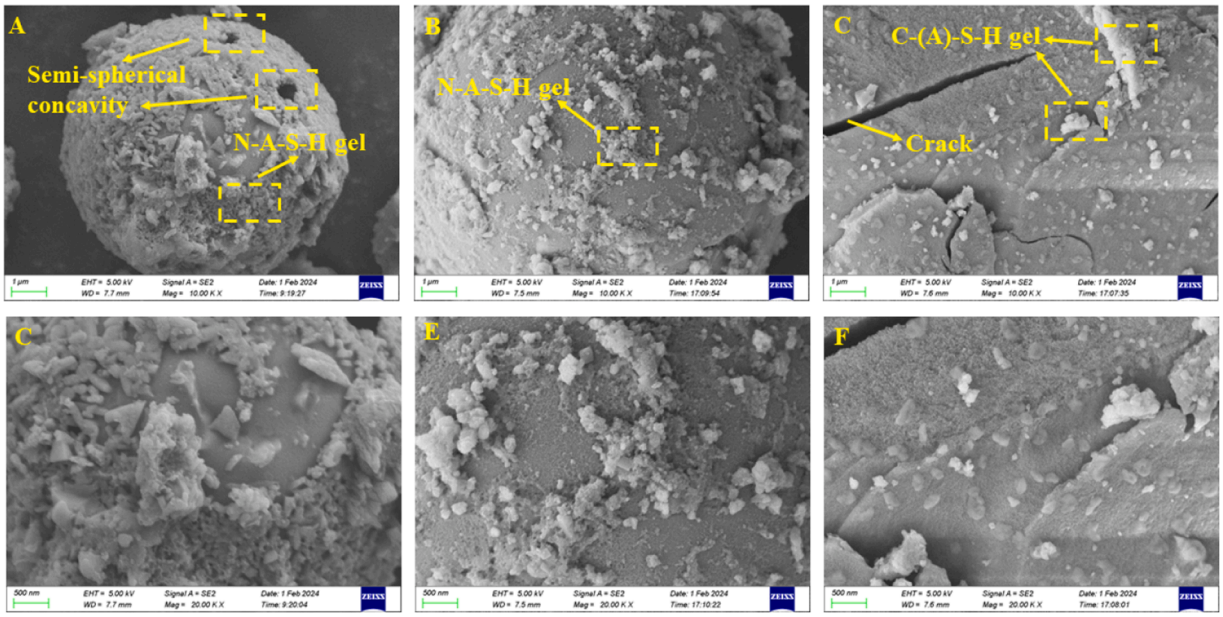

Fig. 4. SEM images of geopolymer samples. FG: (A), (D); SFG: (B); (E); SG: (C), (F).

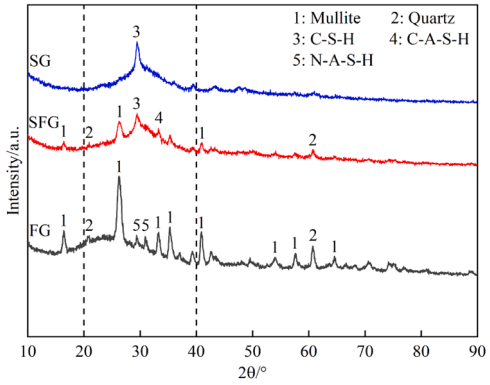

Fig. 5. XRD patterns of samples.

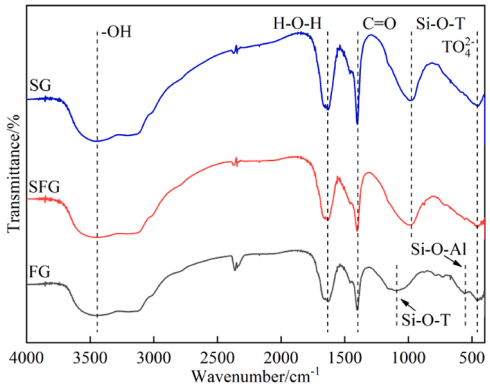

Fig. 6. FTIR spectrum of geopolymer samples. (T=Si or Al).

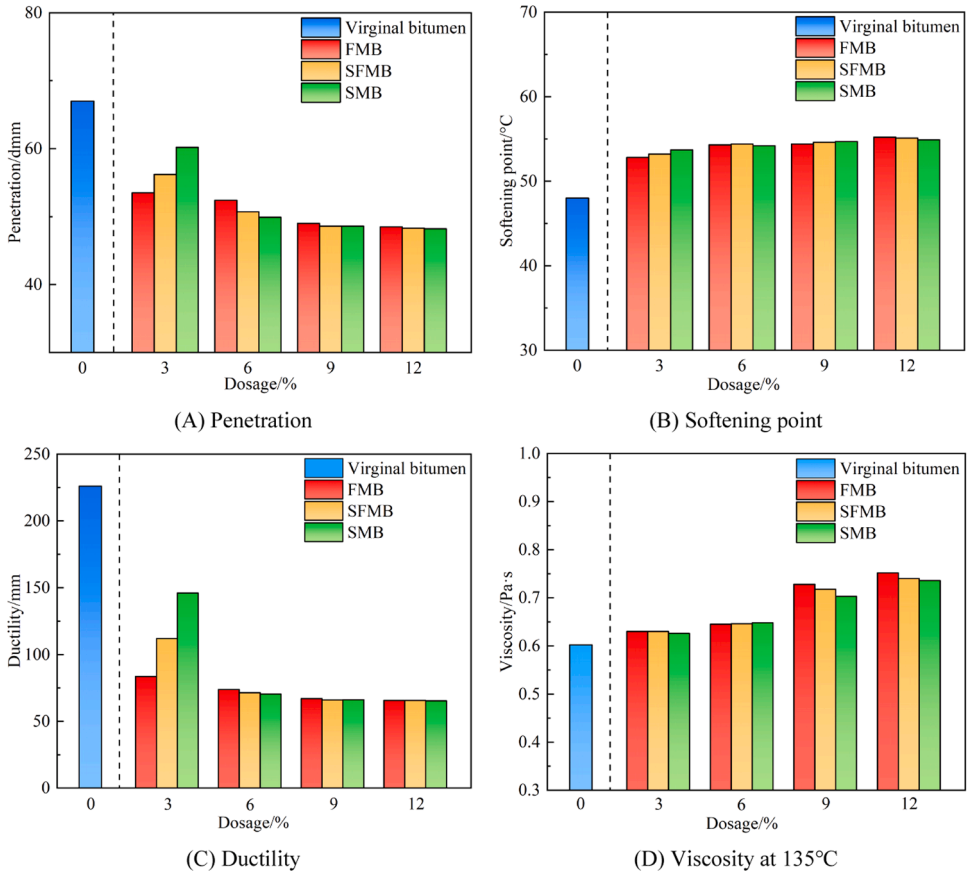

Fig. 7. Properties of modified bitumen.

and softening point. It can be seen from Fig. 4(D) that the viscosity of modified bitumen at 135℃ gradually increased with the increasing addition.

FA and GGBFS generated a large amount of C-(A)-S-H gel and N-A-S-H gel when the alkali activator was added. The C-(A)-S-H gel and N-A-S-H gel were wrapped on the surface of FA and GGBFS particles, which increased the specific surface area of geopolymer. When the geopolymer was added to the bitumen, the surface of geopolymer absorbed a large amount of bitumen and formed structural bitumen, the free bitumen decreased [41]. Therefore, the fluidity of the modified bitumen decreased and the plasticity increased. The penetration and ductility of geopolymer modified bitumen decreased significantly, and the softening point and viscosity increased with the increasing dosage of geopolymer. The high temperature performance of modified bitumen increased and the low temperature performance decreased significantly [42].

3.2.2. Rheological properties of modified bitumen

Complex modulus (G*), phase angle (δ), and rutting factor are shown in Fig. 8, Fig. 9, and Fig. 10 for FMB, SFMB, and SMB respectively.

The complex modulus (G*) of modified bitumen are displayed in Fig. 8. The complex modulus of modified bitumen increased with the increasing addition, in addition, the complex modulus gradually decreased and tended to zero with the increasing temperature. This indicates that the ability to resist deformation increases when geopolymer is added to bitumen.

The phase angle of modified bitumen reflects the relative values of viscous and elastic deformation in modified bitumen [43]. Fig. 9 shows that the phase angle of modified bitumen decreases significantly compared to virginal bitumen and increases with increasing temperature. This indicates that the viscous proportion of bitumen decreases, the elastic percentage increases, and the irrecoverable deformation of the bitumen to resist loading decreases with the addition of geopolymer.

The rutting factor of modified bitumen was calculated according to rutting factor = G*/sinδ [44]. Fig. 10 shows the rutting factor of modified bitumen. As can be seen from Fig. 10, the rutting factor of bitumen increased with the increasing geopolymer and decreased with the increasing temperature [43].

3.2.3. FTIR

Fig. 11 displays the FTIR spectra of bitumen. The FTIR spectra of bitumen did not change significantly with the addition of FG, SFG,

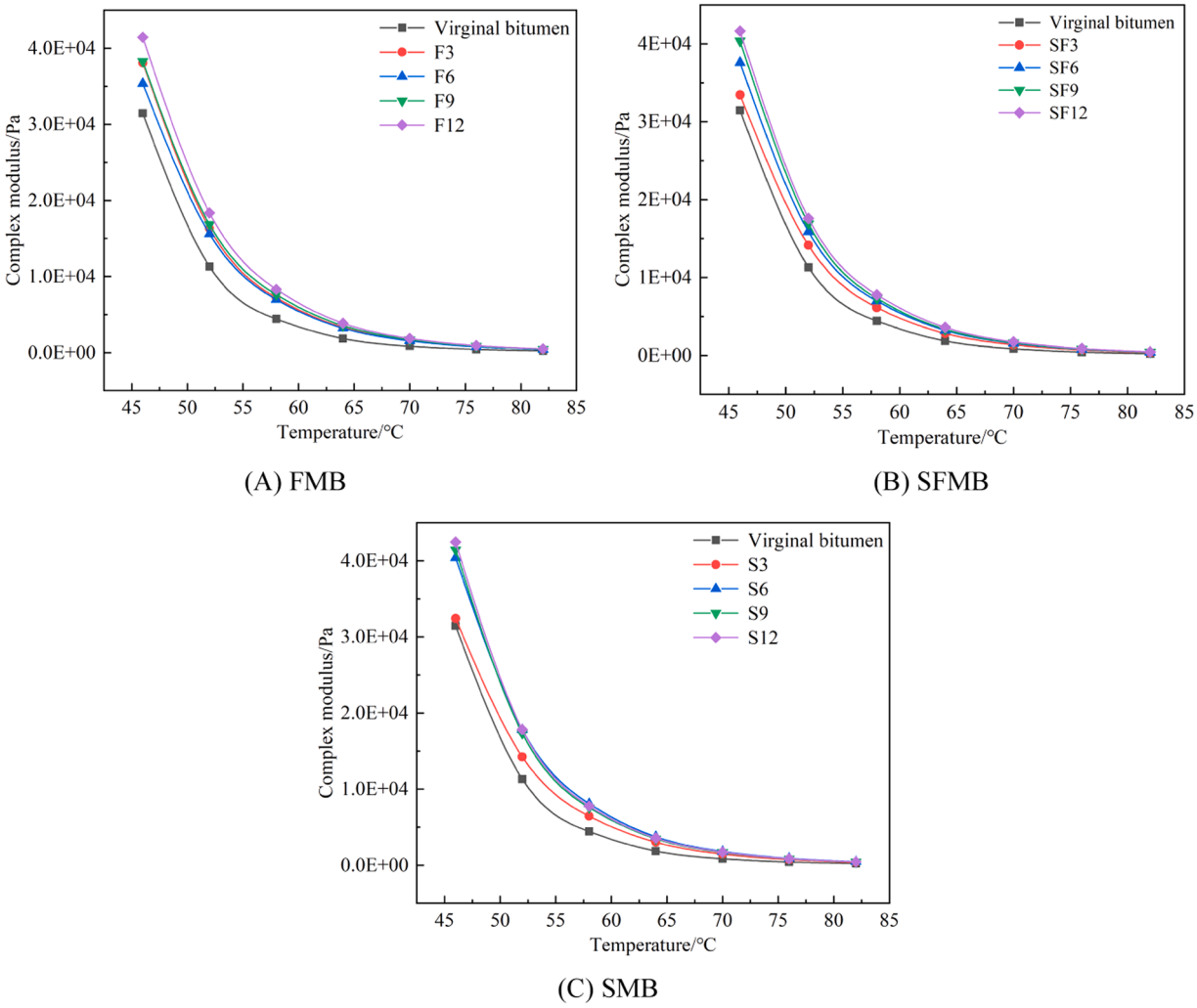

Fig. 8. Complex modulus of modified bitumen.

and SG. This suggests that the addition of geopolymer to bitumen is mainly physical blending accompanied by weak chemical reactions [20].

3.3. Adhesion of bitumen to aggregates

3.3.1. Zeta potential

Fig. 12 displays the Zeta potential of FG, SFG and SG at different pH values. The Zeta potential of FG was negative (-10.51 mv) at pH=3 and decreased gradually with the increasing pH. When pH=3, the Zeta potential of SFG and SG were positive (SFG: 0.31 mv, SG: 2.62 mv). The Zeta potential of SFG and SG were −23.42 mv and −20.67 mv respectively, which indicated that there was an isoelectric point at $3 < pH < 5$, where the dispersion of SFG and SG was poor. The absolute value of Zeta potential is FG > SFG > SG when $pH < 7$, which indicates that FG particles have better dispersion in asphalt.

When the alkaline activator was mixed with FA and GGBFS, the Al-O and Si-O covalent bonds in FA and GGBFS were broken and formed $[AlO_4]^{4-}$ tetrahedra and $[SiO_4]^{4-}$ tetrahedra, and formed a three-dimensional network gel through condensation reactions [45]. In the atomic skeletal structure, metal cations (Na^+, Ca^{2+}) existed to balance the negative charges in the skeletal structure of geopolymer and promote the formation of N-A-S-H gel and C-(A)-S-H gel [46]. Nevertheless, there was a large amount of CaO in GGBFS reacted rapidly to form $Ca(OH)_2$ and C-(A)-S-H gel, which wrapped around the surface of FA and GGBFS particles, blocking the dissolution of reactive Al_2O_3 and SiO_2, and affecting the progress of geopolymer reaction and the formation of N-A-S-H gel when alkali activator was mixed with GGBFS [47,48]. Hence, the amount of N-A-S-H gel in different geopolymer was FG > SFG > SG. Furthermore, the N-A-S-H gel in FG had excellent high temperature stability, however, the C-(A)-S-H gel in SFG and SG was easily decomposed at high temperatures [49–51]. Therefore, the C-(A)-S-H gel in SFG and SG decomposed during high temperature dehydration, the amount of Ca^{2+} decreased, whereas the N-A-S-H gel did not decompose easily and the amount of Na^+ remained constant [52–54].

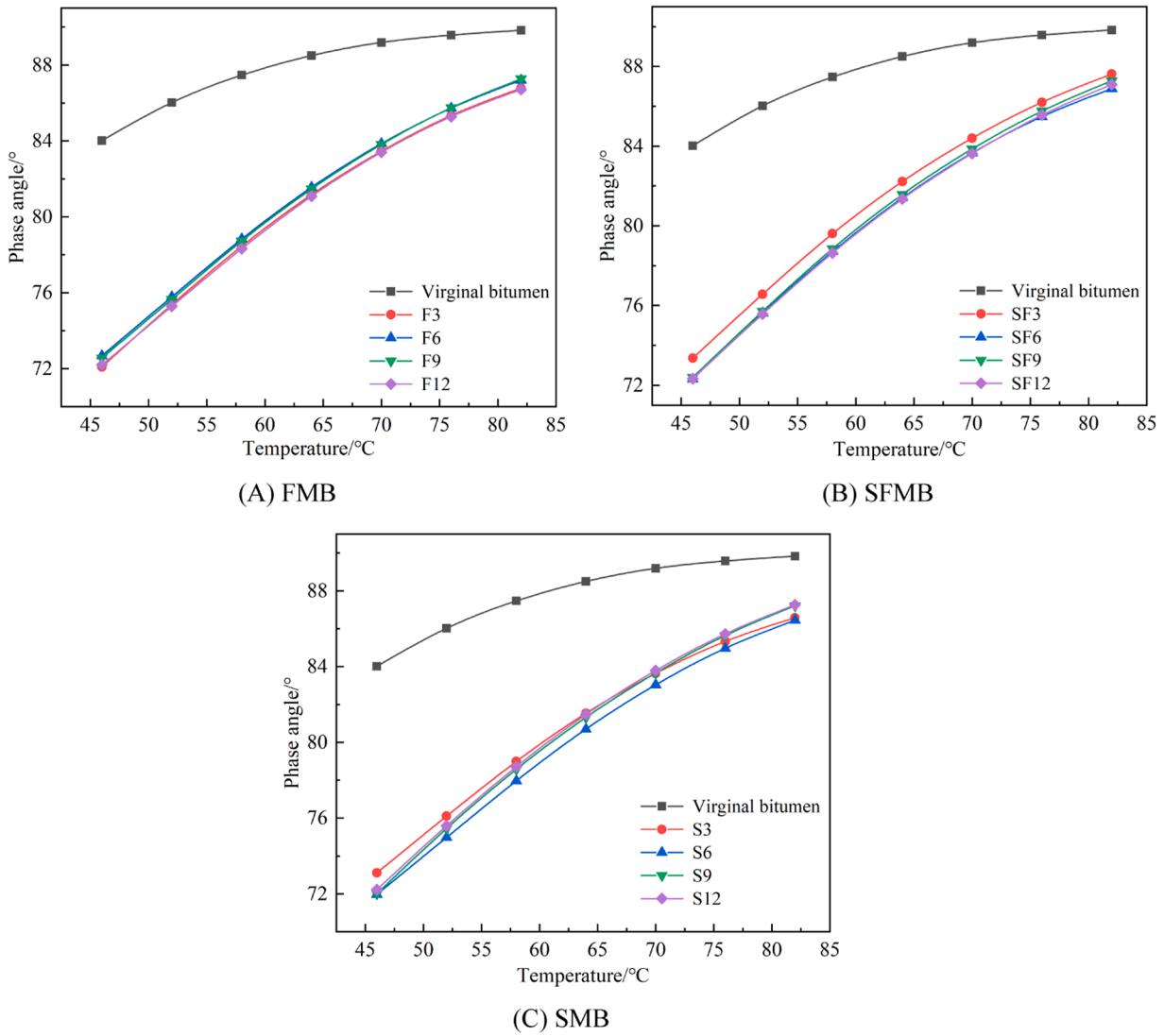

Fig. 9. Phase angle of modified bitumen.

Consequently, the number of metal cations contain in the geopolymer was FG > SFG > SG.

The Zeta potential of bitumen and acidic aggregates is negative, and hence the adhesion of bitumen to acidic aggregates is weak. The mental cations (Na^+, Ca^{2+}) in geopolymer bound to the negative charges in the asphalt and acidic aggregates through electrostatic forces, compressing the double electric and decreasing the electronegativity of the bitumen to the acidic aggregates when FG, SFG, and SG are added to the bitumen [55]. Furthermore, a large quantity of FG particles was wrapped around the surface of acidic aggregates when acidic aggregates was immersed in FMB, and the N-A-S-H gel on the surface of FG particles bonded to bitumen tightly by Coulomb force. As a result, the adhesion of bitumen to acidic aggregates was enhanced. C-(A)-S-H gel in SFG and SG decomposed at high temperature and the amount of Ca^{2+} decreased dramatically, FG contained more metal cations compared to SFG and SG, thus the reduction of electronegativity of bitumen with acidic aggregates was more pronounced. Therefore, the addition of FG improved the adhesion of bitumen to acidic aggregates better.

3.3.2. Boiling water test

The adhesion between modified bitumen and acidic aggregates reflects the mechanical properties of bituminous mixtures [56]. The improved boiling water test and the pull-off test were conducted to analyze the adhesion of different modified bitumen with acidic aggregates.

Fig. 13 shows the results of the improved boiling water test. Table 4 shows the adhesion area of modified bitumen to acidic aggregates. In Fig. 13 and Table 4, the adhesion between virginal bitumen and acidic aggregates is poor. This is due to virginal bitumen stripped with acidic aggregates under the attack of water, as the acidic aggregates contained a large amount of SiO_2, which adsorbed

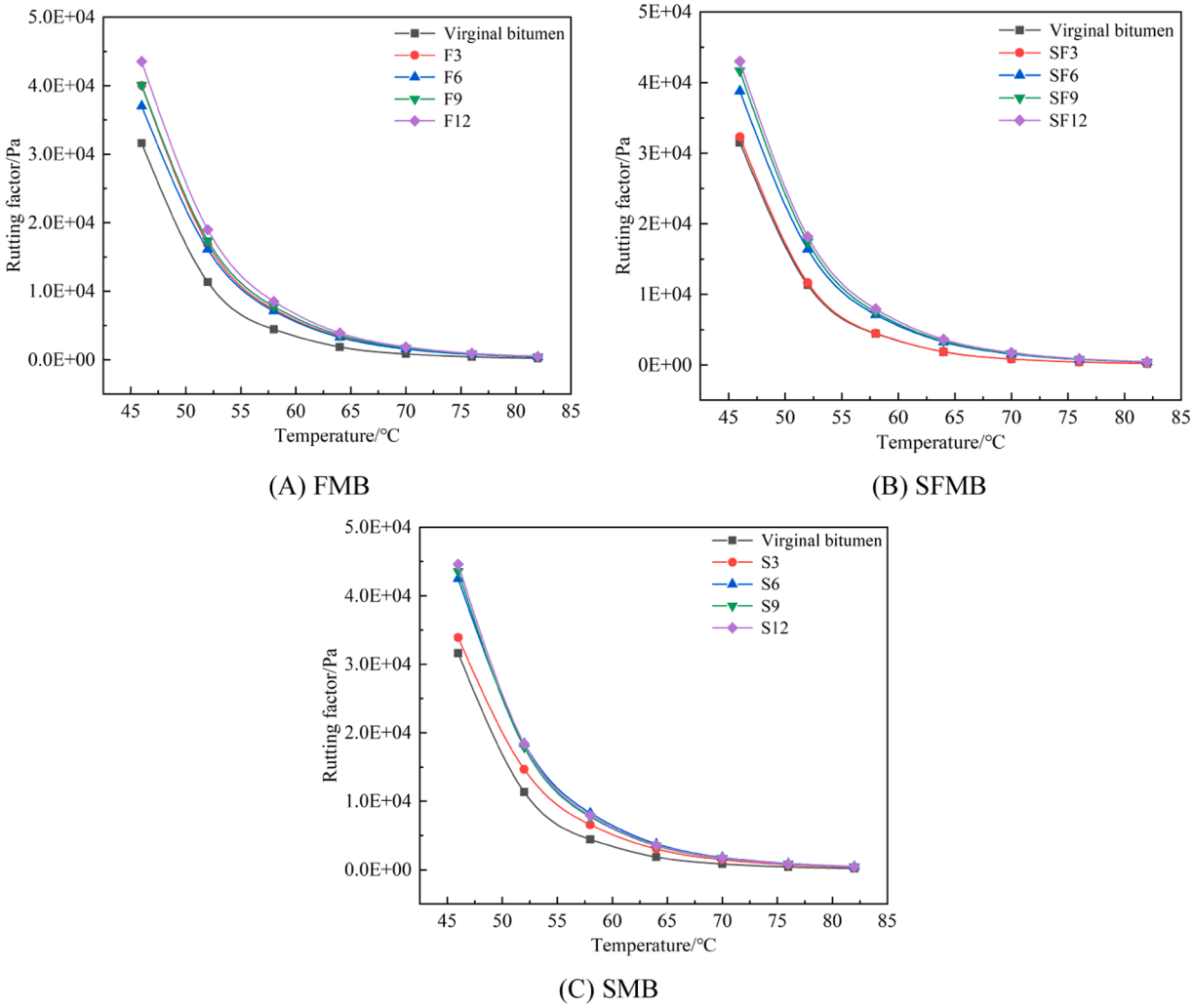

Fig. 10. Rutting factor of modified bitumen.

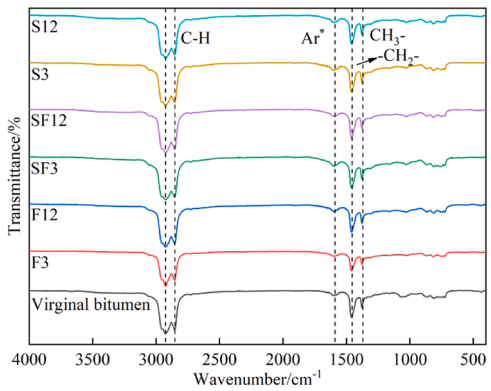

Fig. 11. FTIR spectrum of bitumen.

water easily. The adhesion of bitumen to acidic aggregates increased significantly with the addition of geopolymer. When the dosage was 9 %, FMB, SFMB, and SMB had the most adhesion area with acidic aggregates of 94.27 %, 91.98 % and 91.25 %, respectively, and the adhesion area was enhanced by 126.61 %, 121.11 % and 119.35 % compared to the virginal bitumen, respectively. When the

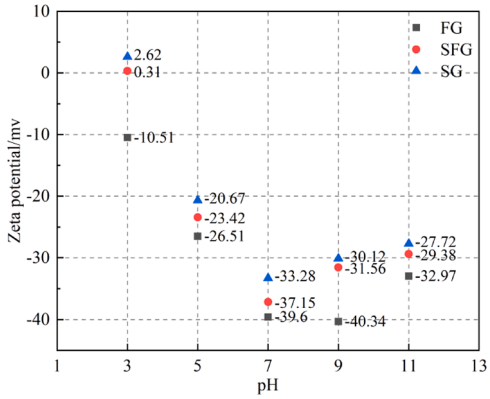

Fig. 12. Zeta potential of geopolymer at different pH values.

geopolymer was added to the bitumen, C-(A)-S-H gel and N-A-S-H gel contained in FG, SFG, and SG adsorbed the bitumen. In addition, the carboxyl (-COOH) in bitumen lost hydrogen atoms and combined with metal cations (Na^+, Ca^{2+}) in geopolymer to form asphaltene that was insoluble in water and distributed on the surface of the acidic aggregates, which enhanced the adhesion of the modified bitumen to the acidic aggregates [42]. However, the adhesion area of modified bitumen to acidic aggregates decreased when the dosage of geopolymer was 12 %. This was due to the many geopolymer particles and the bitumen was not enough adsorbed on the surface of geopolymer particles [57].

According to the results of the improved boiling water test, the adhesion area of different bitumen is FMB > SFMB > SMB. This suggests that N-A-S-H gel in FG can enhance the adhesion of bitumen to acidic aggregates remarkably compared to C-(A)-S-H gel.

3.3.3. Pull-off test

Fig. 14 displays the load-displacement curves of pull-off test for FMB, SFMB, and SMB. Table 5 shows the fracture energy results from FMB, SFMB, and SMB. The load-displacement curves were divided into two phases "rise-decline". When the displacement increased, the load rose sharply and the specimen broke when the load reached the maximum destructive force. Then, the curves decreased sharply and the load was close to zero.

The area enclosed by load-displacement curves was the fracture energy of the specimen and the fracture energy of different curves was calculated by Origin. Table 5 shows that the fracture energy of FMB, SFMB, and SMB with acidic aggregates increases gradually with increasing dosage and reaches the maximum fracture energy at 9 % with the magnitude of FMB > SFMB > SMB. This was because N-A-S-H gel in FG did not decompose while C-(A)-S-H gel in SFG and SG decompose easily at high temperature. Therefore, FG contained more metal cations (Na^+) which weakened the electronegativity of bitumen and acidic aggregates and enhanced the adhesion of bitumen and acid aggregates. When dosage of geopolymer was 12 %, the content of geopolymer was relatively high. There was not enough bitumen to be adsorbed by the geopolymer, resulting in relatively little structural bitumen. Moreover, too much geopolymer added to bitumen tended to clump. Therefore, the adhesion of bitumen to acidic aggregates decreased with 12 % geopolymer dosage.

Fig. 15 shows the fracture surface of pull-off test. Cohesive failure means that the adhesive force between bitumen and aggregates is more than the cohesive force, and the failure internally; the adhesive failure means that the adhesive force between bitumen and aggregates is less than the cohesive force, and the failure at the interface of bitumen and aggregates [32,58]. From Fig. 12, virginal bitumen with acidic aggregates showed adhesive failure in fracture surface which reduced the fracture energy in pull-off test. However, the fracture surface was dominated by cohesive failure when geopolymer was added to virginal bitumen.

3.4. Analyses of cost and environment

At present, the following methods are used for the application of acidic aggregates in asphalt mixtures. (1) Cement is used to replace the mineral powder in the asphalt mixtures. (2) Anti-stripping agent (amine anti-spalling agent) are added to the bitumen. The addition of geopolymer to bitumen improves the adhesion of bitumen to acidic aggregates and reduces costs compared to conventional methods. Table 6 displays the overview of Anti-stripping agent, the cost of anti-stripping agent added per 1 t of asphalt mixtures. In addition, the production of cement generates large quantities of air pollutants (particulate matter, nitrogen oxides, SO_2), as well as vast quantities of greenhouse gases (CO_2). Amine anti-stripping agents require chemical synthesis. The production of geopolymer from solid waste (GGBFS, FA) reduces the emissions CO_2 by about 80 % compared to cement production [59]. Therefore, the enhancement of bitumen adhesion to acidic aggregates by addition geopolymer is economically and ecologically.

4. Conclusions

The adhesion of different modified bitumen (FMB, SFMB, and GMB) with acidic aggregates was investigated in this study. The following conclusions can be drawn based on the above results:

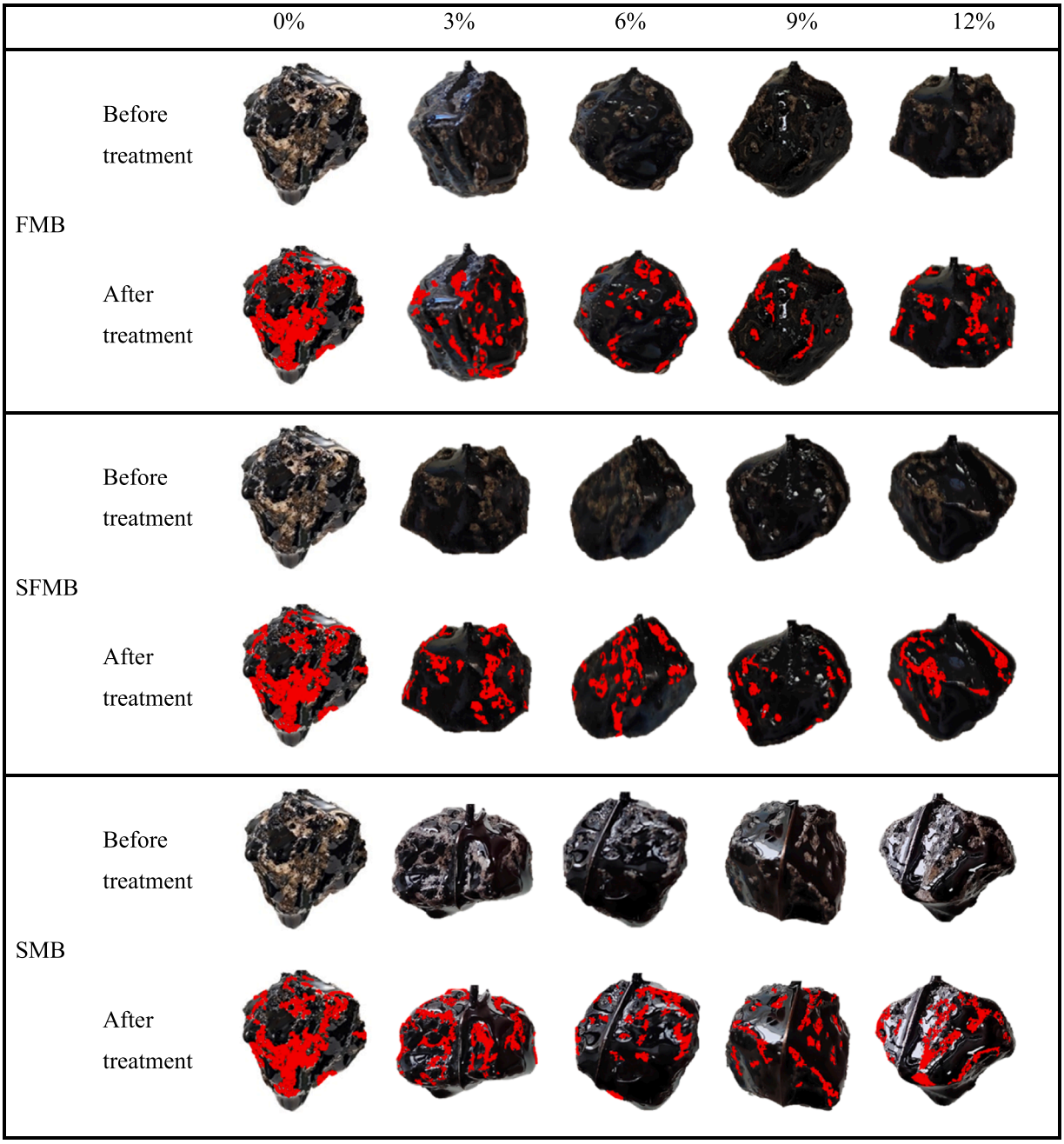

Fig. 13. Results of the boiling water test for modified bitumen and acidic aggregates.

Table 4
Adhesion area of modified bitumen to acidic aggregates tested by the boiling water test.

Dosage	0 %	3 %	6 %	9 %	12 %
FMB	41.60 %	87.44 %	91.42 %	94.27 %	90.73 %
SFMB		86.10 %	89.75 %	91.98 %	88.17 %
SMB		85.58 %	90.63 %	91.25 %	87.15 %

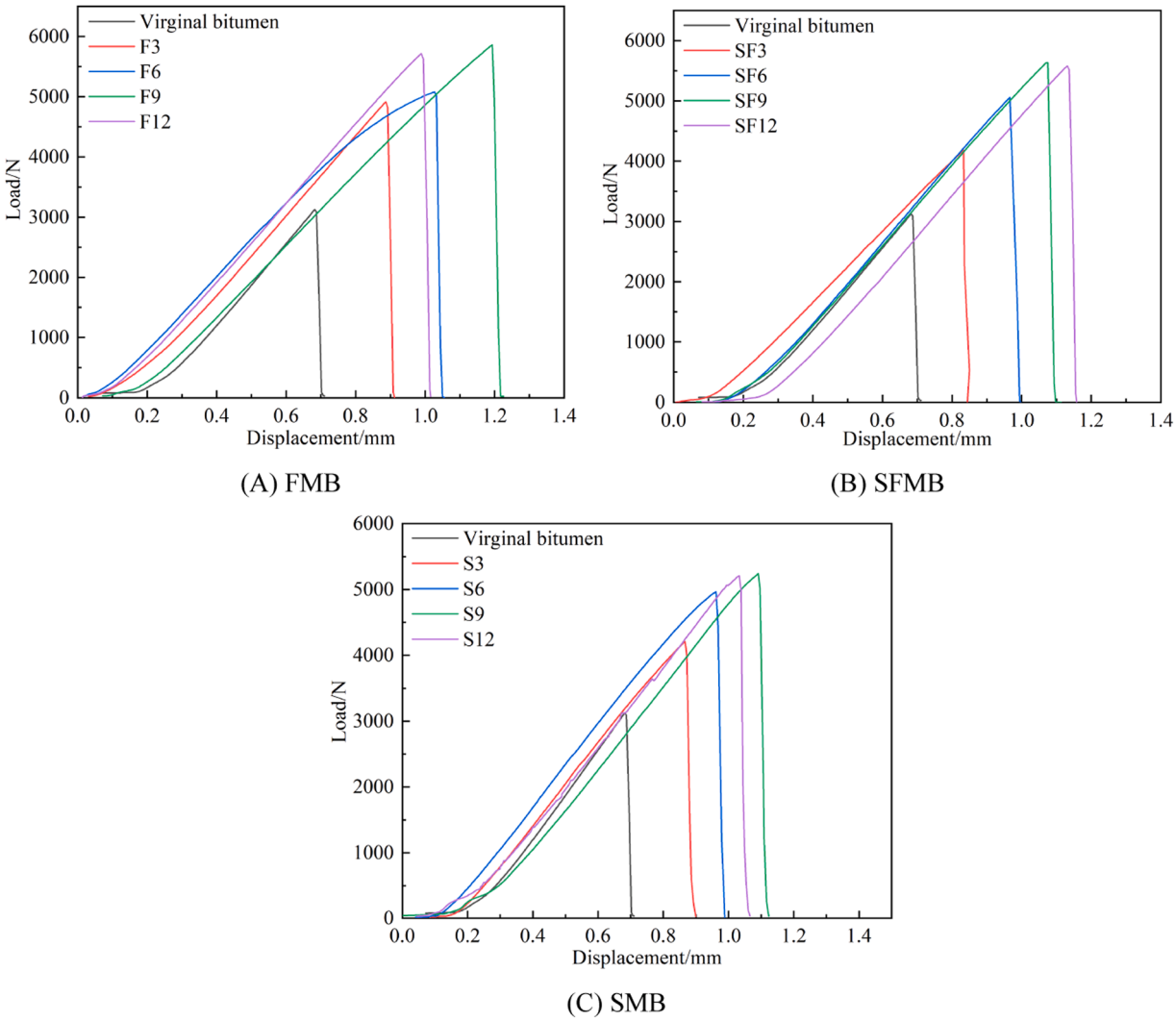

Fig. 14. Load-displacement curves of different modified bitumen.

Table 5
Fracture energy results from different modified bitumen (N·mm).

Dosage	0 %	3 %	6 %	9 %	12 %
FMB	725.85	1866.88	2712.38	3076.70	2577.70
SFMB		1519.83	1961.71	2565.00	2408.56
SMB		1489.26	2164.50	2325.49	2026.92

(1) The addition of alkali activator to FA and GGBFS promoted the formation of geopolymer. A large amount of C-(A)-S-H gel and N-A-S-H gel wrapped around the surface of FA and GGBFS particles were characterized by microscopic.

(2) The addition of geopolymer to bitumen improved the high temperature stability while low temperature performance decreased. The softening point and viscosity increased and the ductility and penetration decreased significantly.

(3) Na^{+} in skeletal structure of FG weakened the electronegativity of bitumen with acidic aggregates. The adhesion of bitumen to acidic aggregates enhanced significantly after the improved boiling water test and pull-off test. The magnitude of bond strength between different bitumen and acidic aggregates were FMB > SFMB > SMB > virginal bitumen.

(4) The addition of geopolymer to bitumen to enhance the adhesion of bitumen to acidic aggregates has enormous economic and environment value.

To further improve the universality of this study, the adhesion of geopolymer modified bitumen with different acidic aggregates will be analysed. Moreover, the pavement performance and durability of geopolymer modified asphalt mixtures with acidic aggregates

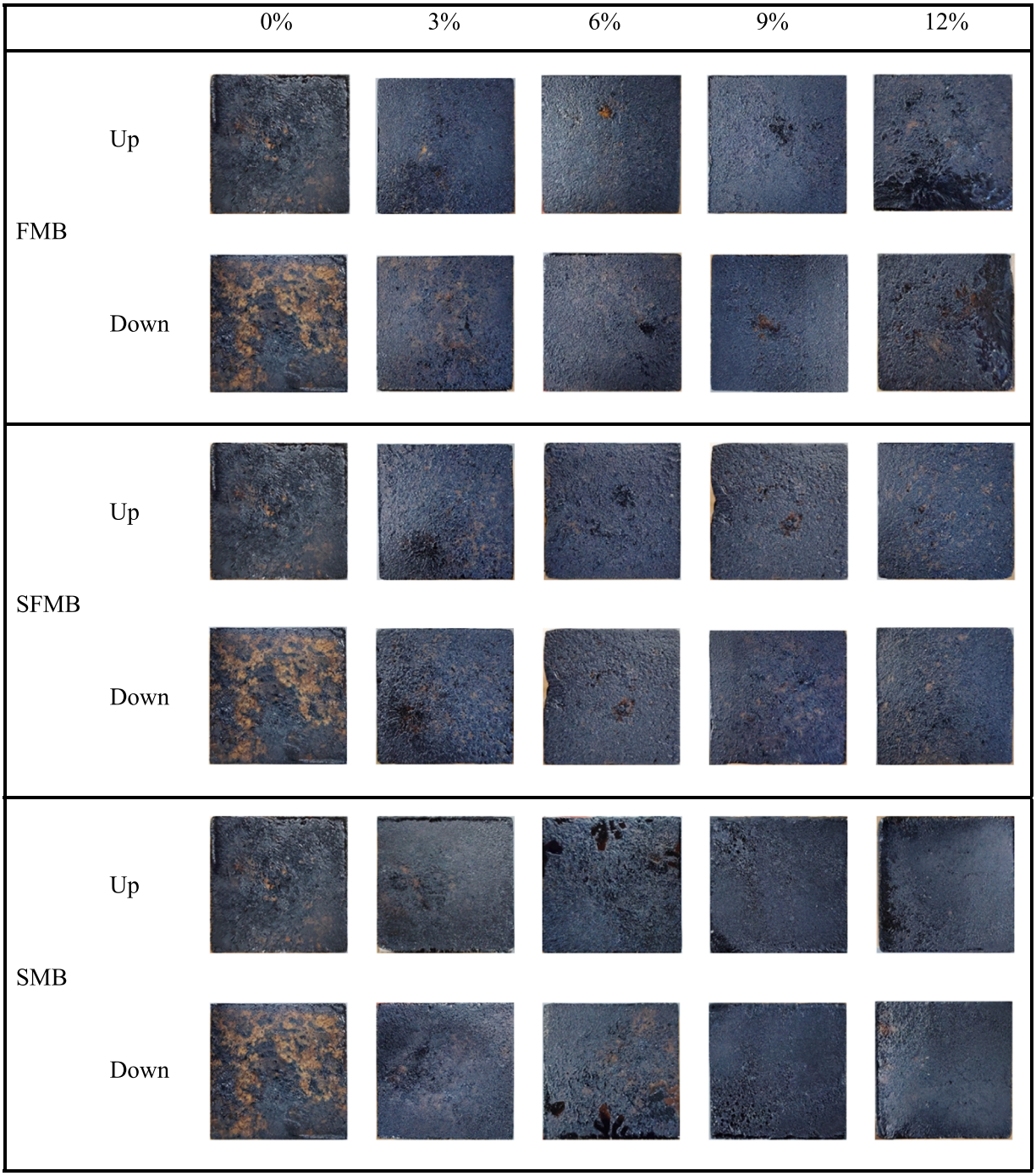

Fig. 15. Fracture surface of pull-off test.

Table 6
Overview of Anti-stripping agent (Average price in market).

Additives	Preparation	State	Cost
Geopolymer	Alkali activation	Solid (powder)	$1.44–2.07
Cement	Synthesis	Solid (powder)	$1.08–2.70
Amine antistripping agents	Synthesis	Liquid	$4.02–6.34

will be explored in future research.

CRediT authorship contribution statement

Nie Nan: Validation, Formal analysis. **Yihan Sun:** Writing – review & editing, Supervision. **Ning Tang:** Writing – original draft, Software, Methodology, Investigation, Conceptualization. **Wenjie Du:** Visualization, Validation, Software, Formal analysis. **Ke Wang:** Writing – review & editing, Supervision, Data curation. **Ruofei Zhang:** Validation, Software, Data curation.

Declaration of Competing Interest

The authors declare that they have no known competing financial interests or personal relationships that could have appeared to influence the work reported in this paper.

Acknowledgements

This work was supported by the Natural Science Foundation of China with grant number 52278453; the Natural Science Foundation of Liaoning with grant number 2024-MS-116; and the Liaoning Revitalization Talents Program with grant number XLYC2007176.

Data Availability

Data will be made available on request.

References

[1] M. Sukhija, V.P. Wagh, N. Saboo, Development of workability based approach for assessment of production temperatures of warm mix asphalt mixtures, Constr. Build. Mater. 305 (2021) 124808, https://doi.org/10.1016/j.conbuildmat.2021.124808.
[2] G. Huang, J. Zhang, Z. Wang, F. Guo, Y. Li, L. Wang, Y. He, Z. Xu, X. Huang, Evaluation of asphalt-aggregate adhesive property and its correlation with the interaction behavior, Constr. Build. Mater. 374 (2023) 130909, https://doi.org/10.1016/j.conbuildmat.2023.130909.
[3] H.-C. Dan, L.-H. He, J.-F. Zou, L.-H. Zhao, S.-Y. Bai, Laboratory study on the adhesive properties of ice to the asphalt pavement of highway, Cold Reg. Sci. Technol. (2014) 104–105, https://doi.org/10.1016/j.coldregions.2014.04.002.
[4] D. Kong, Y. Xiao, S. Wu, N. Tang, J. Ling, F. Wang, Comparative evaluation of designing asphalt treated base mixture with composite aggregate types, Constr. Build. Mater. 156 (2017) 819–827, https://doi.org/10.1016/j.conbuildmat.2017.09.020.
[5] S.N. Sakthivel, A. Kathuria, B. Singh, Utilization of inferior quality aggregates in asphalt mixes: A systematic review, J. Traffic Transp. Eng. Engl. Ed. 9 (2022) 864–879, https://doi.org/10.1016/j.jtte.2022.03.001.
[6] D. Ioannidou, G. Meylan, G. Sonnemann, G. Habert, Is gravel becoming scarce? Evaluating the local criticality of construction aggregates, Resour. Conserv. Recycl. 126 (2017) 25–33, https://doi.org/10.1016/j.resconrec.2017.07.016.
[7] K. Kanitpong, N. Charoentham, S. Likitlersuang, Investigation on the effects of gradation and aggregate type to moisture damage of warm mix asphalt modified with Sasobit, Int. J. Pavement Eng. 13 (2012) 451–458, https://doi.org/10.1080/10298436.2011.565058.
[8] J. Zhang, X. Li, G. Liu, J. Pei, Effects of material characteristics on asphalt and filler interaction ability, Int. J. Pavement Eng. 20 (2019) 928–937, https://doi.org/10.1080/10298436.2017.1366765.
[9] F. Guo, J. Pei, J. Zhang, B. Xue, G. Sun, R. Li, Study on the adhesion property between asphalt binder and aggregate: A state-of-the-art review, Constr. Build. Mater. 256 (2020), https://doi.org/10.1016/j.conbuildmat.2020.119474.
[10] C. Gorkem, B. Sengoz, Predicting stripping and moisture induced damage of asphalt concrete prepared with polymer modified bitumen and hydrated lime, Constr. Build. Mater. 23 (2009) 2227–2236, https://doi.org/10.1016/j.conbuildmat.2008.12.001.
[11] L. Mo, M. Huurman, S. Wu, A.A.A. Molenaar, Ravelling investigation of porous asphalt concrete based on fatigue characteristics of bitumen–stone adhesion and mortar, Mater. Des. 30 (2009) 170–179, https://doi.org/10.1016/j.matdes.2008.04.031.
[12] V. Najafi Moghaddam Gilani, G.H. Hamedi, M.R. Esmaeeli, M. Habibzadeh, M. Hosseinpour Eshkiknezhad, Presentation of thermodynamic and dynamic modules methods to investigate the effect of nano hydrated lime on moisture damage of stone matrix asphalt, Aust. J. Civ. Eng. 21 (2023) 141–150, https://doi.org/10.1080/14488353.2022.2083404.
[13] T. Schlegel, D. Puiatti, H.-J. Ritter, D. Lesueur, C. Denayer, A. Shtiza, The limits of partial life cycle assessment studies in road construction practices: a case study on the use of hydrated lime in Hot Mix Asphalt, Transp. Res. Part Transp. Environ. 48 (2016) 141–160, https://doi.org/10.1016/j.trd.2016.08.005.
[14] H. Sun, Y. Ding, P. Jiang, B. Wang, A. Zhang, D. Wang, Study on the interaction mechanism in the hardening process of cement-asphalt mortar, Constr. Build. Mater. 227 (2019), https://doi.org/10.1016/j.conbuildmat.2019.08.044.
[15] S. Zarei, J. Ouyang, W. Yang, Y. Zhao, Experimental analysis of semi-flexible pavement by using an appropriate cement asphalt emulsion paste, Constr. Build. Mater. 230 (2020) 116994, https://doi.org/10.1016/j.conbuildmat.2019.116994.
[16] E. Hesami, G. Mehdizadeh, Study of the amine-based liquid anti-stripping agents by simulating hot mix asphalt plant production process, Constr. Build. Mater. 157 (2017) 1011–1017, https://doi.org/10.1016/j.conbuildmat.2017.09.168.
[17] Y. Peng, Z. Yu, Y. Long, Y. Li, Experimental investigation on the effects of a new anti-stripping additive on performance properties of asphalt and its mixtures, Constr. Build. Mater. 353 (2022) 129173, https://doi.org/10.1016/j.conbuildmat.2022.129173.
[18] M. Yu, T. Wang, Y. Chi, D. Li, L. Li, F. Shi, Residual mechanical properties of GGBS-FA-SF blended geopolymer concrete after exposed to elevated temperatures, Constr. Build. Mater. 411 (2024) 134378, https://doi.org/10.1016/j.conbuildmat.2023.134378.
[19] S.A.P. Rosyidi, S. Rahmad, N.I.M.D. Yusoff, A.H. Shahrir, A.N.H. Ibrahim, N.F.N. Ismail, K.H. Badri, Investigation of the chemical, strength, adhesion and morphological properties of fly ash based geopolymer-modified bitumen, Constr. Build. Mater. 255 (2020) 119364, https://doi.org/10.1016/j.conbuildmat.2020.119364.
[20] Y. Meng, J. Lei, R. Zhang, X. Yang, Q. Zhao, Y. Liao, Y. Hu, Effect of geopolymer as an additive on the mechanical performance of asphalt, Road. Mater. Pavement Des. 23 (2022) 2466–2485, https://doi.org/10.1080/14680629.2021.1977169.
[21] X. Ge, X. Hu, H. Li, C. Shi, Synergistic effect of characteristics of raw materials on controlling the mechanical properties of fly ash-based geopolymers, Cem. Concr. Compos. 145 (2024) 105368, https://doi.org/10.1016/j.cemconcomp.2023.105368.
[22] X. Li, C. Bai, Y. Qiao, X. Wang, K. Yang, P. Colombo, Preparation, properties and applications of fly ash-based porous geopolymers: A review, J. Clean. Prod. 359 (2022) 132043, https://doi.org/10.1016/j.jclepro.2022.132043.

[23] Z. Qiu, S. Bao, Y. Zhang, M. Huang, C. Lin, X. Huang, Y. Chen, Y. Ping, Effect of Portland cement on the properties of geopolymers prepared from granite powder and fly ash by alkali-thermal activation, J. Build. Eng. 76 (2023) 107363, https://doi.org/10.1016/j.jobe.2023.107363.
[24] C. Yang, J.-J. You, Y.-W. Huang, X.-M. Ji, Q.-Y. Song, Q. Liu, Low-carbon enhancement of fly ash geopolymer concrete: Lateral deformation, microstructure evolution and environmental impact, J. Clean. Prod. 422 (2023) 138610, https://doi.org/10.1016/j.jclepro.2023.138610.
[25] K.M. Klima, K. Schollbach, H.J.H. Brouwers, Q. Yu, Thermal and fire resistance of Class F fly ash based geopolymers – A review, Constr. Build. Mater. 323 (2022) 126529, https://doi.org/10.1016/j.conbuildmat.2022.126529.
[26] R.P. Singh, K.R. Vanapalli, K. Jadda, B. Mohanty, Durability assessment of fly ash, GGBS, and silica fume based geopolymer concrete with recycled aggregates against acid and sulfate attack, J. Build. Eng. 82 (2024) 108354, https://doi.org/10.1016/j.jobe.2023.108354.
[27] N. Shehata, O.A. Mohamed, E.T. Sayed, M.A. Abdelkareem, A.G. Olabi, Geopolymer concrete as green building materials: Recent applications, sustainable development and circular economy potentials, Sci. Total Environ. 836 (2022) 155577, https://doi.org/10.1016/j.scitotenv.2022.155577.
[28] C. Chen, K. Sasaki, Q. Tian, H. Zhang, Fabrication of one-part geopolymer from coal gasification slag via alkali fusion and component additive method: Effect of different alkali-to-slag ratios, J. Build. Eng. 80 (2023) 107938, https://doi.org/10.1016/j.jobe.2023.107938.
[29] J. Zhang, M. Chen, S. Wu, D. Chen, Y. Zhao, X. Zhou, Characteristics of waste dry battery powder and its enhancement effect on the physicochemical properties of asphalt binder, J. Clean. Prod. 426 (2023) 139090, https://doi.org/10.1016/j.jclepro.2023.139090.
[30] J. Fan, Y. Zhu, T. Ma, G. Xu, X. Ding, Interface interaction between high viscosity asphalt and aggregate: A multi-scale study based on experiments and molecular dynamics simulation, Fuel 357 (2024) 130045, https://doi.org/10.1016/j.fuel.2023.130045.
[31] J. Zhang, A.K. Apeagyei, G.D. Airey, J.R.A. Grenfell, Influence of aggregate mineralogical composition on water resistance of aggregate–bitumen adhesion, Int. J. Adhes. Adhes. 62 (2015) 45–54, https://doi.org/10.1016/j.ijadhadh.2015.06.012.
[32] Y. Wu, X. Zhu, C. Liu, Z. Dai, Assessment of interfacial fracture of asphalt mortar-aggregate system at low temperature: A study based on four-point bending test of sandwich beams, Constr. Build. Mater. 352 (2022) 129057, https://doi.org/10.1016/j.conbuildmat.2022.129057.
[33] B. Ma, Z. Zhu, W. Huo, L. Yang, Y. Zhang, H. Sun, X. Zhang, Assessing the viability of a high performance one-part geopolymer made from fly ash and GGBS at ambient temperature, J. Build. Eng. 75 (2023) 106978, https://doi.org/10.1016/j.jobe.2023.106978.
[34] C. Gunasekara, D.W. Law, S. Setunge, J.G. Sanjayan, Zeta potential, gel formation and compressive strength of low calcium fly ash geopolymers, Constr. Build. Mater. 95 (2015) 592–599, https://doi.org/10.1016/j.conbuildmat.2015.07.175.
[35] B. Xing, Y. Du, C. Fang, H. Sun, Y. Lyu, W. Fan, Particle morphology of mineral filler and its effects on the asphalt binder-filler interfacial interaction, Constr. Build. Mater. 321 (2022) 126292, https://doi.org/10.1016/j.conbuildmat.2021.126292.
[36] X. Ge, X. Hu, C. Shi, Impact of micro characteristics on the formation of high-strength Class F fly ash-based geopolymers cured at ambient conditions, Constr. Build. Mater. 352 (2022) 129074, https://doi.org/10.1016/j.conbuildmat.2022.129074.
[37] T. H.M, S. Unnikrishnan, Mechanical Strength and Microstructure of GGBS-SCBA based Geopolymer Concrete, J. Mater. Res. Technol. 24 (2023) 7816–7831, https://doi.org/10.1016/j.jmrt.2023.05.051.
[38] A. Elimbi, H.K. Tchakoute, D. Njopwouo, Effects of calcination temperature of kaolinite clays on the properties of geopolymer cements, Constr. Build. Mater. 25 (2011) 2805–2812, https://doi.org/10.1016/j.conbuildmat.2010.12.055.
[39] M. Xia, F. Muhammad, L. Zeng, S. Li, X. Huang, B. Jiao, Y. Shiau, D. Li, Solidification/stabilization of lead-zinc smelting slag in composite based geopolymer, J. Clean. Prod. 209 (2019) 1206–1215, https://doi.org/10.1016/j.jclepro.2018.10.265.
[40] J. He, T. Guo, Z. Li, Y. Gao, J. Zhang, Hydration mechanism of red mud-fly ash based geopolymer, Mater. Chem. Phys. 314 (2024) 128807, https://doi.org/10.1016/j.matchemphys.2023.128807.
[41] K. Yan, L. Li, kaigao Zheng, D. Ge, Research on properties of bitumen mortar containing municipal solid waste incineration fly ash, Constr. Build. Mater. 218 (2019) 657–666, https://doi.org/10.1016/j.conbuildmat.2019.05.151.
[42] E.G. Bautista, J. Flickinger, R. Saha, I. Flores-Vivian, A.F. Faheem, K. Sobolev, Effect of Coal Combustion Products on high temperature performance of asphalt mastics, Constr. Build. Mater. 94 (2015) 572–578, https://doi.org/10.1016/j.conbuildmat.2015.07.022.
[43] P. Xu, Z. Chen, J. Cai, J. Pei, J. Gao, J. Zhang, J. Zhang, The effect of retreated coal wastes as filler on the performance of asphalt mastics and mixtures, Constr. Build. Mater. 203 (2019) 9–17, https://doi.org/10.1016/j.conbuildmat.2019.01.088.
[44] X. Ren, A. Sha, J. Li, W. Jiang, W. Jiao, W. Wu, X. Ling, Carbon fiber powder in sustainable asphalt pavements: Improving microwave self-healing capacity and low-temperature performance, J. Clean. Prod. 440 (2024) 140828, https://doi.org/10.1016/j.jclepro.2024.140828.
[45] L. Jia-Ni, L. Yun-Ming, H. Cheng-Yong, T. Wei-Hong, P. Wei Ken, P. Pakawanit, T. Hoe-Woon, H. Yong-Jie, O. Shee-Ween, O. Wan-En, Unveiling physico-mechanical and acoustical characteristics of fly ash geopolymers through the synergistic impact of density and porosity, J. Build. Eng. 91 (2024) 109684, https://doi.org/10.1016/j.jobe.2024.109684.
[46] N.F. Shahedan, T. Hadibarata, M.M.A.B. Abdullah, M.N.H. Jusoh, S.Z.A. Rahim, I. Isia, A.A. Bras, A. Bouaissi, F.H. Juwono, Potential of fly ash geopolymer concrete as repairing and retrofitting solutions for marine infrastructure: a review, Case Stud. Constr. Mater. 20 (2024) e03214, https://doi.org/10.1016/j.cscm.2024.e03214.
[47] M.M. Madirisha, O.R. Dada, B.D. Ikotun, Chemical fundamentals of geopolymers in sustainable construction, Mater. Today Sustain. 27 (2024) 100842, https://doi.org/10.1016/j.mtsust.2024.100842.
[48] H. Lin, J. Zhang, R. Wang, W. Zhang, J. Ye, Adsorption properties and mechanisms of geopolymers and their composites in different water environments: A comprehensive review, J. Water Process Eng. 62 (2024) 105393, https://doi.org/10.1016/j.jwpe.2024.105393.
[49] M. Chen, D. Wu, K. Chen, P. Cheng, Y. Tang, The influence of fly ash-based geopolymer on the mechanical properties of OPC-solidified soil, Constr. Build. Mater. 432 (2024) 136591, https://doi.org/10.1016/j.conbuildmat.2024.136591.
[50] F. Li, Y. Wang, L. Ma, B. Li, J. Wei, Q. Yu, J. Jiang, Synthesis and characterization of hierarchical porous slag-based geopolymers by ice-templating method, Constr. Build. Mater. 433 (2024) 136726, https://doi.org/10.1016/j.conbuildmat.2024.136726.
[51] S. Janga, A.N. Raut, A.L. Murmu, Assessment of thermal and mechanical properties of fly ash based geopolymer blocks with a sustainability perspective using multi-criteria decision-making approach, J. Build. Eng. 88 (2024) 109261, https://doi.org/10.1016/j.jobe.2024.109261.
[52] A.M. Mhaya, S. Shahidan, A. Goel, G.F. Huseien, Effect of metakaolin content and shape design on strength performance of lightweight rubberized geopolymer mortars incorporated slag-waste glass powders, Constr. Build. Mater. 432 (2024) 136500, https://doi.org/10.1016/j.conbuildmat.2024.136500.
[53] B. Nanda, J. Mishra, S.K. Patro, Synthesis of rice husk ash based alkaline activators for geopolymer binder systems: A review, J. Build. Eng. 91 (2024) 109694, https://doi.org/10.1016/j.jobe.2024.109694.
[54] H. Li, X. Guo, Corrosion resistance and mechanisms of class C fly ash-based geopolymer in simulated oil well environments: Mud contamination and salt solutions at high temperature, Constr. Build. Mater. 424 (2024) 135917, https://doi.org/10.1016/j.conbuildmat.2024.135917.
[55] Y. Zhang, M. Ding, J. Liu, W. Jia, S. Ren, Studies on bitumen–silica interaction in surfactants and divalent cations solutions by atomic force microscopy, Colloids Surf. Physicochem. Eng. Asp. 482 (2015) 241–247, https://doi.org/10.1016/j.colsurfa.2015.05.012.
[56] H. Ren, Z. Qian, B. Lin, Q. Huang, M. Crispino, M. Ketabdari, Effect of recycled concrete aggregate features on adhesion properties of asphalt mortar-aggregate interface, Constr. Build. Mater. 353 (2022) 129097, https://doi.org/10.1016/j.conbuildmat.2022.129097.
[57] X. Sun, Z. Ou, T. Zhao, X. Qin, J. Jin, H. Yu, L. Li, Interaction state and element leaching of waste incineration fly ash-asphalt mortar based on fillerization, Constr. Build. Mater. 398 (2023) 132463, https://doi.org/10.1016/j.conbuildmat.2023.132463.
[58] S. Ling, D. Jelagin, D. Sun, H. Fadil, Experimental and numerical analyses on the fracture characteristics of cement-asphalt mastic-aggregate interface, Constr. Build. Mater. 401 (2023) 132971, https://doi.org/10.1016/j.conbuildmat.2023.132971.
[59] Y. Ding, J.-G. Dai, C.-J. Shi, Mechanical properties of alkali-activated concrete: a state-of-the-art review, Constr. Build. Mater. 127 (2016) 68–79, https://doi.org/10.1016/j.conbuildmat.2016.09.121.